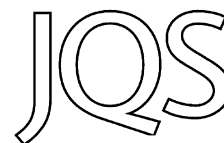


# Chronostratigraphic constraints on Middle Pleistocene faunal assemblages and Acheulian industries from the Cretone lacustrine basin, central Italy



FABRIZIO MARRA,<sup>1\*</sup> PIERO CERULEO,<sup>2</sup> BRIAN JICHA,<sup>3</sup> LUCA PANDOLFI,<sup>4</sup> CARMELO PETRONIO,<sup>5</sup> LEONARDO SALARI,<sup>5</sup> BIAGIO GIACCIO<sup>6</sup> and GIANLUCA SOTTILI<sup>6</sup>

<sup>1</sup>Istituto Nazionale di Geofisica e Vulcanologia, Sezione Roma 1, Via di Vigna Murata 605, 00147 Roma, Italy

<sup>2</sup>Via Giotto 18, 00019 Tivoli (Roma), Italy

<sup>3</sup>Department of Geoscience, University of Wisconsin-Madison, 1215 W. Dayton Street, Madison, WI 53706, USA

<sup>4</sup>Dipartimento di Scienze, sezione di Geologia, Università degli Studi "Roma Tre", Largo S. Leonardo Murialdo 1, 00146 Rome, Italy

<sup>5</sup>Dipartimento di Scienze della Terra, Sapienza, Università di Roma, Piazzale Aldo Moro 5, 00185 Rome, Italy

<sup>6</sup>Istituto di Geologia Ambientale e Geoingegneria – CNR, Via Salaria km 29, 300, 00015 Montelibretti (Rome), Italy

Received 25 August 2015; Revised 10 June 2016; Accepted 29 June 2016

**ABSTRACT:** Integrated <sup>40</sup>Ar/<sup>39</sup>Ar, trace-element, stratigraphic, palaeontological and palaeoethnological data provide geochronological and biochronological constraints for the sedimentary and tectonic history of a Middle Pleistocene fluvial–lacustrine basin near Rome (Cretone Basin, central Italy), which has yielded a significant record of mammal fossil remains and Palaeolithic industry. This work is a case study of the interplay between tectonics and glacio-eustasy, which strongly influenced the evolution of the Tyrrhenian Sea margin of central Italy. Dating of tephra layers interbedded within the Cretone Basin lacustrine succession and reconstruction of relict terraced surfaces allow correlation with similar, geochronologically constrained, marine isotopic stages (MIS) 15–5 terraced deposits along the coast. Coupled extensional tectonics and regional uplift over the last 600 ka caused the progressive uplifting and westward migration of the main fluvial–lacustrine basin and the formation of a smaller satellite basin at its eastern margin. Here, stable environmental conditions during MIS 13–5 indicated continuous human and large mammal frequentation, as testified by lithic industry and fossil remains ascribable to the Acheulean and later early Middle Palaeolithic technocomplexes and Galerian–Aurelian mammal faunas, respectively. In addition to providing independent age constraints to glacial sea-level oscillations of this region, the reconstructed chronostratigraphic setting for the Cretone Basin provides evidence for one of the oldest Acheulean lithic assemblage of central Italy, as well as new biochronological and palaeobiogeographical data for some Middle Pleistocene mammal species of Italy. Copyright © 2016 John Wiley & Sons, Ltd.

**KEYWORDS:** <sup>40</sup>Ar/<sup>39</sup>Ar dating; aggradational successions; glacio-eustatic cycles; Lower Palaeolithic lithic industry; Middle Pleistocene vertebrate fauna; peri-Tyrrhenian–Quaternary basin; Sabatini Volcanic District; tectonism; terraces; trace element analysis.

## Introduction

Reconstructing the sedimentary–geomorphological evolution of Quaternary basins in continental margin settings facilitates an evaluation of the role of the underlying processes responsible for their formation, which are mainly related to glacio-eustatic oscillations, vertical and/or differential volcano-tectonic movements, and their mutual interplay. It can also improve general knowledge of the extinction and occurrence events of Quaternary large mammals, the duration of coexistence of different species as well as their relation/interference with climatic changes and with Palaeolithic communities. Using new stratigraphic, palaeontological, palaeoethnological, geochemical, <sup>40</sup>Ar/<sup>39</sup>Ar geochronological data, and comprehensive geomorphological/structural analysis, the peri-Tyrrhenian Cretone Basin, Tiber Valley, central Italy (Fig. 1), has been investigated. Through the systematic determination of the large number of vertebrate fossil remains and Palaeolithic industry collected in the Cretone Basin (Fig. 1), in combination with morphostratigraphic and geochronological information, we frame the faunal assemblages and related lacustrine deposits within the newly acquired biochronological outline for the Middle Pleistocene faunal units of Italy (Marra *et al.*, 2014a). Following the tephra fingerprinting approach proposed by Marra *et al.* (2014a) for the adjacent Sabatini Volcanic District,

the recognized fluvial–lacustrine morpho-sedimentary units, belonging to the hydrographic network of the Tiber River, and the related faunal assemblages, are correlated to glacio-eustatic sea-level fluctuations, and thus attributed to the marine isotopic stage successions.

## Geological setting

The investigated area (Fig. 1a) is located at the north-eastern edge of the Tyrrhenian Sea margin of central Italy, at the back of the Apennine orogenic belt (Doglioni *et al.*, 1999, and references therein). This sector was affected by back-arc extension after Messinian times, culminating in the subduction-related, ultrapotassic volcanism of the Roman Comagmatic Region during the Middle Pleistocene (Peccerillo, 2005, and references therein). The sedimentary processes in this area, which led to the deposition of ten glacio-eustatically forced aggradational successions over the last 900 ka (Marra *et al.*, 2008, and references therein), were strongly influenced by the interplay between volcanism, tectonics and glacio-eustatism. Several studies (Karner and Marra, 1998; Marra *et al.*, 1998; Florindo *et al.*, 2007) provided a comprehensive geochronological framework linking these aggradational successions to Marine Isotopic Stages (MIS) 21–1. Marra *et al.* (2014a) used these geochronological constraints on the sedimentary deposits of the coastal area of Ponte Galeria (Conato *et al.*, 1980; Milli *et al.*, 2008), in which a large number of

\*Correspondence to: F. Marra, as above.  
E-mail: fabrizio.marra@ingv.it

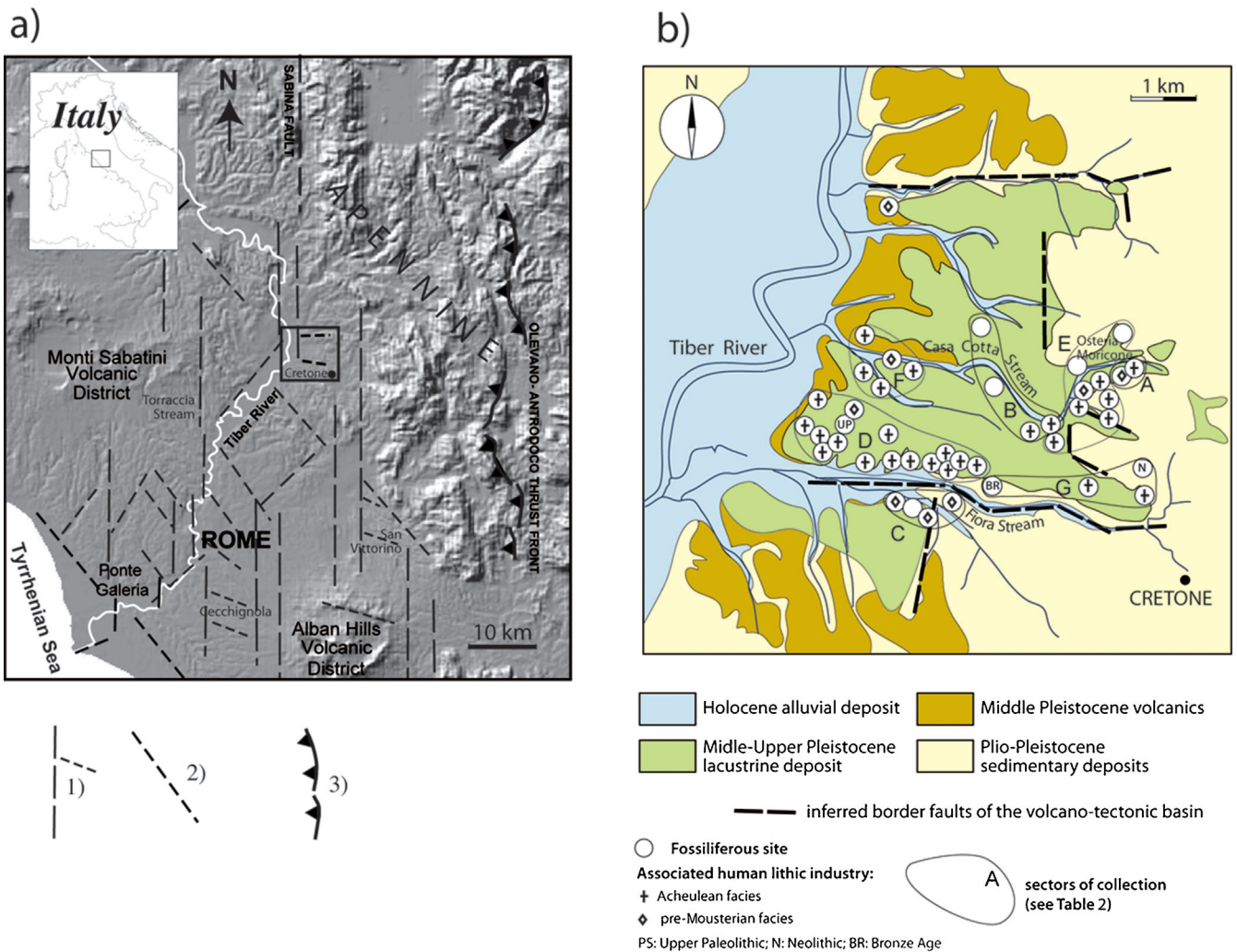


**Figure 1.** (a) Digital elevation model image of the area of Rome, showing the main structural lineaments; (b) geological map of the Cretone Basin, showing the location of the fossiliferous sites described in this paper.

mammal faunas were described (e.g. Gliozzi *et al.*, 1997; Petronio and Sardella, 1999; Milli and Palombo, 2005; Petronio *et al.*, 2011), to re-calibrate the ages of the mammal assemblages and to reconstruct a new biochronological and palaeobiogeographical framework for the Italian Peninsula during the Middle Pleistocene (Fig. 2).

Hitherto, very little is known about the Cretone Basin with available information limited to the Geologic Map of Italy (1 : 100 000 Palombara Sabina sheet 144; Servizio Geologico d'Italia, 1970) and few notes on the stratigraphy of a section containing several vertebrate remains attributed to the Late Galerian or Early Aurelian Mammal Age (Middle Pleistocene), including *Palaeoloxodon antiquus*, *Bos primigenius*, *Dama* sp. and ?*Cervus* sp. (Manni *et al.*, 2000; Di Canzio *et al.*, 2003). Specifically, the 1 : 100 000 geological map reports the presence of a particular lithology in a restricted sector, coinciding with the investigated area where the mammal remains and the human industry were collected. This is reported as 'pedogenized tuffs', as opposed to the primary pyroclastic succession that represents the widespread geological cover, outcropping on top and along the flanks of the hills in this area, which overlies marine clay and sand sediments of Plio-Pleistocene age (Girotti and Mancini, 2003) (Fig. 1b).

### Stratigraphy

Scanty outcrops occur along the gentle flanks of the stream valleys cutting the relatively flat topographic surface within

the Cretone Basin (Fig. 3). However, a few road cuts and anthropic scarps expose a limited portion of the sedimentary fill of the lacustrine basin (sections 1–5 in Figs 3 and 9. More frequently, field ploughing exhumes some of the sedimentary deposits underlying the shallow pedogenized cover, as in the example in Fig. 4(a), or as in Osteria Moricone, where white, well-bedded lacustrine muds with intercalations of decimeter-thick volcanoclastic layers (Fig. 4f) occasionally crop out.

The investigated sections expose bedded sandy clay and sandy silt deposits, with more or less abundant, sparse volcanoclastic sediments, and frequent freshwater *Gastropoda*, indicating a lacustrine environment. Occasionally, as in section 5, the lowest portion of the sedimentary succession is exposed, revealing an overall fining-upward sequence, with coarse, cross-bedded volcanoclastic sand and fine-grained gravel at the base, suggestive of a fluvial environment, followed by silt and clay, diatomitic horizons and travertine layers at the top, attesting to more quiet, lacustrine conditions (Fig. 4b). In other sections (1, 3, 4), primary or sub-primary volcanic deposits are interfingered with clay sediments. In particular, a pumice-fall deposit, which geochemical analyses performed for this work identify as the  $589 \pm 4$  ka FAD-1 eruption unit from the Monti Sabatini district (Marra *et al.*, 2014b), is intercalated in the lowest portion of the lacustrine succession, cropping out at the Montelibretti Station (section 1; Figs 3, 4c and 9). Similarly, the Fall A1 pumice-fall deposit (see geochemical signature in Fig. 8a–a'), dated at  $499 \pm 3$  ka (Marra *et al.*, 2014b), is

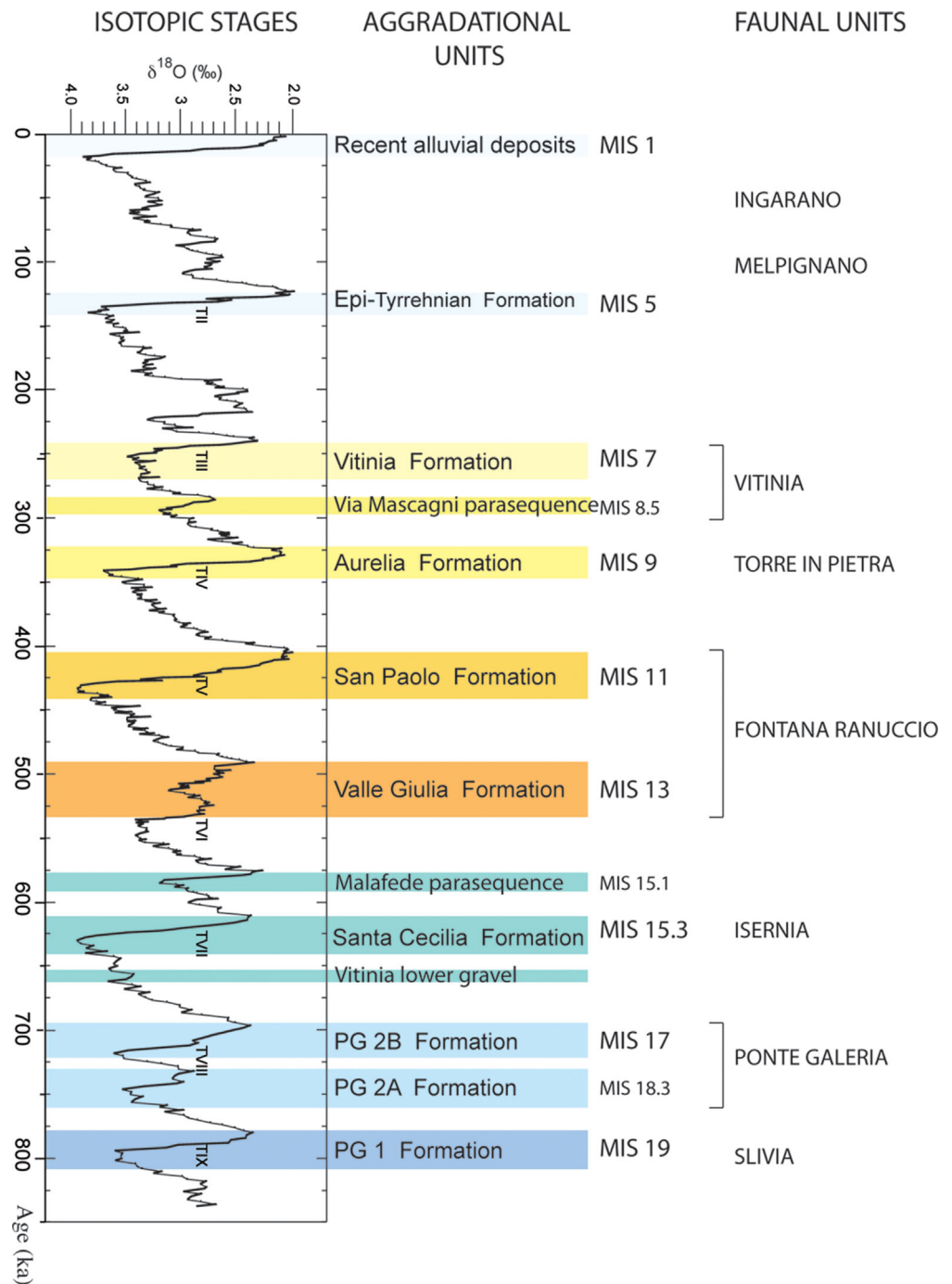


**Figure 2.** Correlation between the marine isotopic stages (MIS), as depicted by the oxygen isotope record (Lisiecki and Raymo, 2005), the aggradational units of the paleo-Tiber River, and the faunal units of the Middle–Upper Pleistocene of Italy (modified from Marra *et al.*, 2014a).

intercalated within a 2-m-thick sandy clay deposit cropping out in the intermediate portion of the lacustrine basin (section 3; Figs 3, 4d and 9).

Overall, the sedimentary features of the deposits representing the infill of the Cretone Basin (upward successions of gravel, sand and clay) and the environmental characterization provided by the abundant freshwater Gastropoda, account for their classification as continental aggradational successions. The age constraints provided by the dated tephra layers establish the synchronicity between their deposition and the timing of sea-level rise during glacial terminations of MIS 15–5 (glacio-eustatic cycles).

## Material and methods

### Morphotectonic investigations

Our morphostructural analyses of the hydrographic network followed the approaches used to reconstruct the structural

setting in different sectors of the larger area of Rome (Caputo *et al.*, 1993; Marra, 2001). Rectified streambed directions are statistically analysed to depict preferential channel orientation; the significant concentrations are considered to match those of the main faults and fractures that controlled the structuration and the geometry of the sedimentary basin as a result of vertical displacement occurring during the regional volcano-tectonic phases.

Terraced surfaces have also been identified and compared to those found in the study performed in the Fosso Galeria area, located near the Tyrrhenian Sea coast south-west of Rome, by Karner *et al.* (2001a).

### Geochronological investigations

To provide geochronological constraints for the investigated lacustrine succession and support correlation to the different marine isotope stages, we performed two  $^{40}\text{Ar}/^{39}\text{Ar}$  age



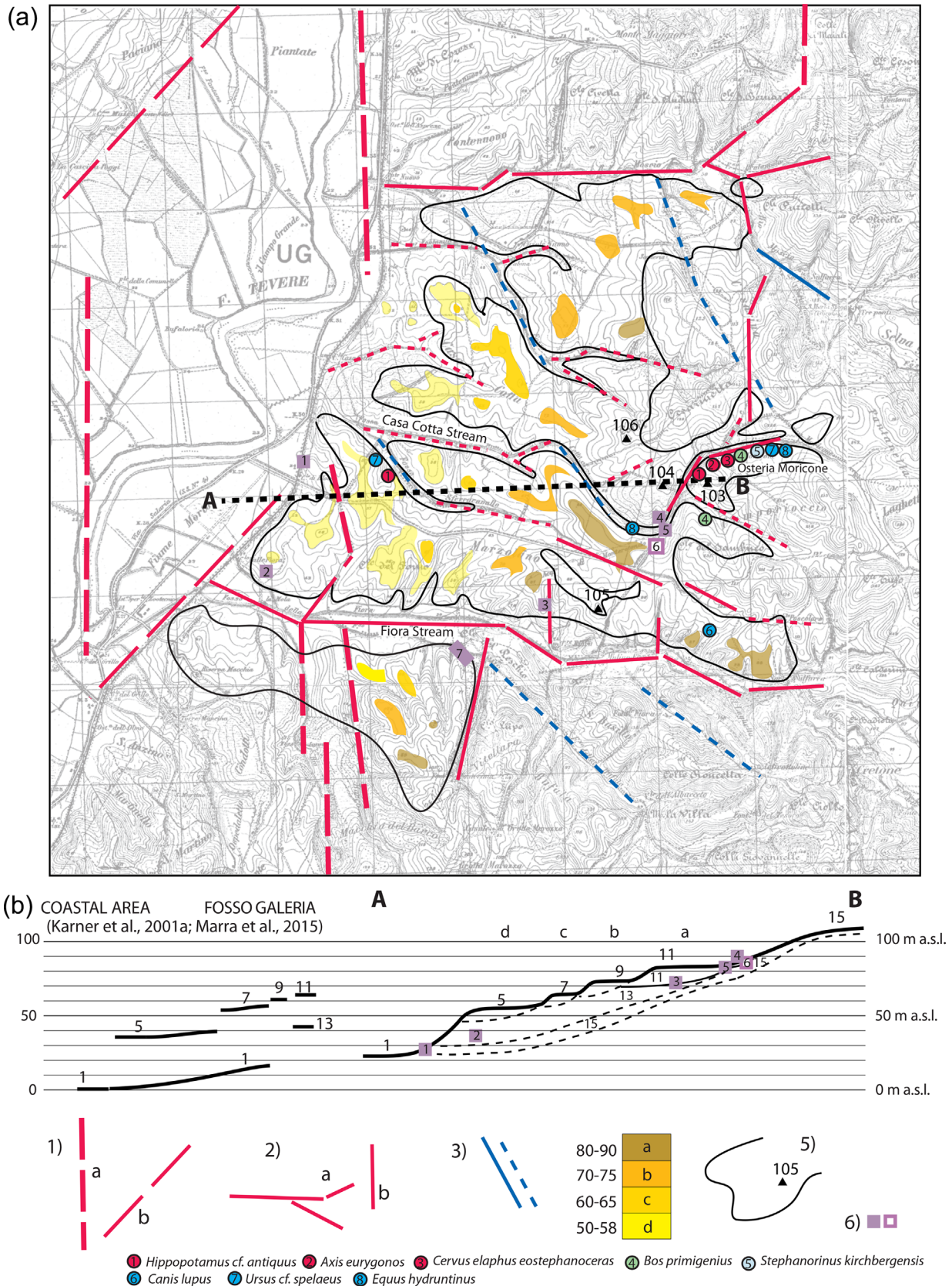


**Figure 3.** (a) Morpho-structural map of the Cretone Basin; (b) cross-section showing elevation of the terraces and the associated lacustrine deposits, and the proposed correlation with the marine isotope stages; comparison with elevation of the geochronologically constrained terraces in the coastal area of this region is also provided. Legend: 1, main N-S fault segments (a) and related transfer faults (b); 2, conjugated system of faults and fractures inferred from the rectified streambed directions (a) and minor N-S fault segments (b): solid lines represent the fault segments experiencing vertical dislocation during formation of the volcano-tectonic basin; 3, NW-SE-trending lineaments matching the direction of the fault system linked to the regional extensional tectonic regime (see text for explanation and references); 4, terraced surfaces and related elevation range of the lacustrine succession; 5, geological limit of the lacustrine deposits and maximum elevation (triangle); 6, location of the stratigraphic sections investigated in this study and of the fossiliferous site reported in Manni *et al.* (2000) (□).



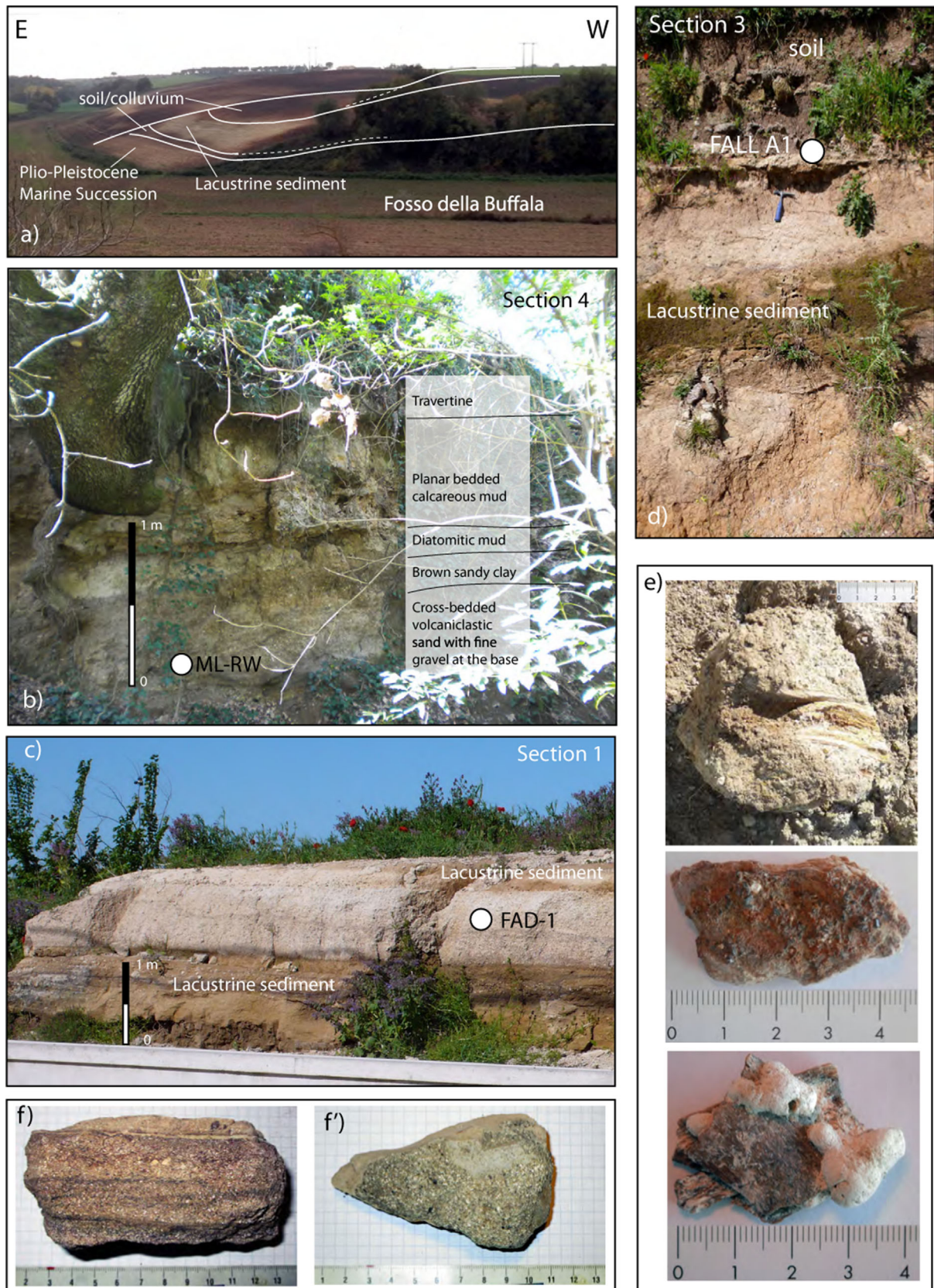


**Figure 4.** (a) Photograph of the north-eastern flanks of Fosso della Buffala (Section 7) showing the stratigraphic context in which the collection of fossils and artefacts was performed; (b) stratigraphic Section 4 exposing a fluvial–lacustrine fining-upward succession, in which sample ML-RW was collected; (c) stratigraphic Section 1 and position of sample FAD-1; (d) stratigraphic Section 3 and position of sample FALL A1; (e) examples of bone fragments coated with lacustrine clayey and volcanoclastic sediment collected in Sferracavallo, Marzolino and Osteria Moricone; (f) volcanoclastic sediment outcropping in Osteria Moricone; (f') bifacial with adhering sediment collected at the same location. See text for details and Fig. 3 for location of the sections.

**Table 1.** Major and selected trace-element fusion-ICP and fusion-MS analyses for four samples collected in the Cretone basin (ML-TG, ML-RL, ML-FAD, ML-FALL A; locations are shown in Fig. 3), and for four samples of primary volcanic deposits collected in the proximal setting of the Sabatini Volcanic District to compare composition of those from Cretone. TGCP-Vm, Tufo Giallo di Castelnuovo di Porto; LTGVT-Si, lower Tufo Giallo della Via Tiberina; TGPP-Gr, Tufo Giallo di Prima Porta (from Grottarossa locality); TGPP-CR, Tufo Giallo dui Prima Porta (from Cava Rinaldi locality) [see Marra *et al.* (2014b) for information about these samples].

Analyte	SiO <sub>2</sub> (%)	Al <sub>2</sub> O <sub>3</sub> (%)	Fe <sub>2</sub> O <sub>3</sub> (T) (%)	MnO (%)	MgO (%)	CaO (%)	Na <sub>2</sub> O (%)	K <sub>2</sub> O (%)	TiO <sub>2</sub> (%)	P <sub>2</sub> O <sub>5</sub> (%)	LOI (%)	Total (%)	Y (p.p.m.)	Zr (p.p.m.)	Nb (p.p.m.)	
Detection limit	0.01	0.01	0.01	0.001	0.01	0.01	0.01	0.01	0.001	0.01	0.01	0.01	0.01	2	4	1
Analysis method	FUS-ICP	FUS-ICP	FUS-ICP	FUS-ICP	FUS-ICP	FUS-ICP	FUS-ICP	FUS-ICP	FUS-ICP	FUS-ICP	FUS-ICP	FUS-ICP	FUS-ICP	FUS-ICP	FUS-ICP	FUS-MS
ML-TG	48.53	25.44	4.23	0.014	0.55	1.04	0.57	1.89	0.873	0.19	14.54	97.87	50	602	47	
ML-RL	30.84	6.51	3.74	0.074	2.1	29.11	0.48	0.94	0.322	0.17	25.07	99.37	17	151	10	
ML-FAD	53.26	18.45	4.24	0.136	0.64	2.73	3.86	2.71	0.493	0.1	11.54	98.15	34	519	26	
ML-FALL A	41.37	19.38	4.49	11.37	0.48	2.28	1.13	1.18	0.524	0.16	14.69	97.05	30	470	34	
TGCP-Vm	50.18	15.32	3.52	0.142	0.98	8.94	2.36	4.46	0.429	0.12	12.06	98.5	28	450	26	
LTGVT-Si	55.52	16.87	3.9	0.12	1.29	2.78	2.46	3.17	0.517	0.14	11.68	98.45	35	462	31	
TGPP-Gr	51.61	18.78	4.59	0.125	1.42	4.78	3.6	5.7	0.481	0.21	7.52	98.82	39	610	46	
TGPP-CR	49.61	14.6	5.88	.007	1.74	9.37	2.46	1.51	0.671	0.32	13.2	99.43	28	292	17	

Full analytical data and quality reports are provided as Online Supplementary Material 3.

determinations and trace-element analyses on four samples of pyroclastic products collected in the field (Supplementary Tables S1 and S2). Moreover, we determined the trace-element bulk composition of three pyroclastic flow deposits erupted during the early activity of the Sabatini Volcanic District to integrate the existing dataset (Sottili *et al.*, 2010; Marra *et al.*, 2014b), and to compare those of the deposits sampled in the Cretone Basin.

### <sup>40</sup>Ar/<sup>39</sup>Ar ages

<sup>40</sup>Ar/<sup>39</sup>Ar dating was performed on sanidine grains extracted from samples ML-FA and ML-RW from primary or reworked pyroclastic deposits (Sections 4 and 5; Fig. 3; see Online Supplementary Material 2 for a description of the samples). Sanidine phenocrysts were isolated from the deposits using standard magnetic and density separation techniques, and were co-irradiated with the 1.186 Ma Alder Creek sanidine standard (Rivera *et al.*, 2013; Jicha *et al.*, 2016) at the Oregon State University TRIGA reactor in the Cadmium-Lined In-Core Irradiation Tube. Single crystal fusion analyses were performed at the WiscAr laboratory at the University of Wisconsin-Madison. Sample ML-FA was analysed using the Noblesse multi-collector mass spectrometer following Jicha *et al.* (2016), and sample ML-RW was analysed using an MAP-215-50 mass spectrometer.

### Geochemical analyses

Four bulk samples of pyroclastic deposits interbedded with lacustrine deposits of the Cretone Basin, plus four samples of as many primary pyroclastic deposits cropping out in the Sabatini Volcanic District, were analysed by lithium metaborate/tetraborate fusion ICP-MS at Activation Laboratories, Ontario, Canada (selected trace-element data are given in Table 1; full geochemical data are provided as Online Supplementary Material 3).

### Palaeontological analyses

In the present work, we classify and describe 210 selected fossil remains (Table 2) among hundreds collected in five distinct sectors of the Cretone Basin (Fig. 1b) and presently housed at the Museo Preistorico del territorio Tiburtino-Cornicolano of Sant'Angelo Romano (Rome, Italy).

The collection of fossil remains and of the lithic industry was carried out in repeated, systematic field surveys at over 30 sites reported in Fig. 1(b). The materials emerge in light-coloured, clayey deposits rich in reworked pyroclastic material along the flanks of the hills, corresponding to the fluvial-lacustrine sediments, which alternate with darker strata (pyroclastic deposits, colluvium and palaeosols) without lithic finds (Fig. 4a).

A number of bone fragments were polished, suggesting abrasion or smoothing due to water transport. However, the selected remains are well preserved and a few of them are complete. Several specimens have a coating of the lacustrine sediment in which they were embedded, accounting for their provenance (Fig. 4d).

A detailed description of the studied specimens is provided in the Online Supplementary Material 4, whereas several taxa providing useful relative age constraints for the identification of the sedimentary cycles are discussed in the following section. The biochronological intervals for the different taxa are mainly based on those reported in Petronio *et al.* (2011) and Marra *et al.* (2014a).

### Archaeological analyses

Study of the lithic industry was carried out according to Bordes' artefact taxonomy for the classification of tools

**Table 2.** Number of identified specimens (NISP) according to the localities within the Cretone Basin (bold: the taxa whose biochronological interval provides age constraints to the investigated lacustrine successions of the Cretone Basin in which the vertebrate remains occur). A, Camporiocchio; B, Fosso Casa Cotta; C, Fosso della Bufala; D, Marzolino; E, Osteria Moricone; F, Sferracavallo; G, Valle Fiora.

Taxon	A	B	C	D	E	F	G	Total
Testudinoidea		1						1
<i>Canis lupus</i>							1	1
<i>Ursus cf. spelaeus</i>					1	1		2
<i>Crocota crocuta</i>	5							5
Elephantidae	5			5		1		11
<i>Palaeoloxodon antiquus</i>	6	1		1	11	2		21
<b><i>Stephanorhinus sp.</i></b>	<b>3</b>	<b>2</b>	<b>1</b>		<b>1</b>	<b>2</b>		<b>9</b>
<b><i>Stephanorhinus cf. kirchbergensis</i></b>				<b>1</b>				<b>1</b>
<b><i>Stephanorhinus kirchbergensis</i></b>		<b>2</b>						<b>2</b>
<i>Equus ferus</i>	5	2		4	11	4		26
<i>Equus hydruntinus</i>					2	1		3
Hippopotamidae						1		1
<i>Hippopotamus cf. antiquus</i>			1		1			2
<i>Sus scrofa</i>					3			3
Megacerinae					1			1
Cervinae	1	2		1	4			8
<i>Axis eurygonos</i>					5			5
<i>Cervus elaphus ssp.</i>	2	1	1	4	18	3		29
<i>Cervus elaphus eastephanoceros</i>					9			9
<i>Dama sp.</i>	1	6	1		13	6		27
<i>Capreolus capreolus</i>		1						1
<i>Bos vel Bison</i>	3		3	5	4	1		16
<i>Bison cf. schoetensacki</i>					1			1
<i>Bison priscus</i>					1			1
<i>Bos primigenius</i>	3		2	3	14	2		24
Total NISP	34	19	9	24	100	23	1	210

(Bordes, 1961) to provide a preliminary description of the types of artefacts recovered at the different sites and to make a comparison with previous studies of Lower Palaeolithic sites in Italy, which were usually conducted according to this methodology. The collected archaeological record consists of more than 1200 artefacts (including 347 instruments, 171 nuclei, 706 flakes); a detailed description of the materials is provided in Ceruleo *et al.* (2015).

## Results

### Morpho-structural and stratigraphic setting

The investigated morpho-sedimentary units occur within a sub-rhomboidal structural depression whose morphological

expression is a gentle, relatively flat landscape bounded by the markedly sharper and higher morphology of the hills carved in marine Plio-Pleistocene deposits (Fig. 3). The basin hosts a fluvial-lacustrine succession, represented by sandy clay deposits with abundant reworked pyroclastic material, which differs substantially from the previously reported lithological unit ('pedogenized tuffs' in the 1 : 100 000 geological map) and whose limits have been slightly modified (Fig. 3).

The basin geometry reflects that of a system of currently inactive faults and fractures, which probably drove the formation and evolution of the Cretone Basin (Fig. 3). In particular, the rectified streambed directions reveal a particular framework (Fig. 5), similar to that described in other

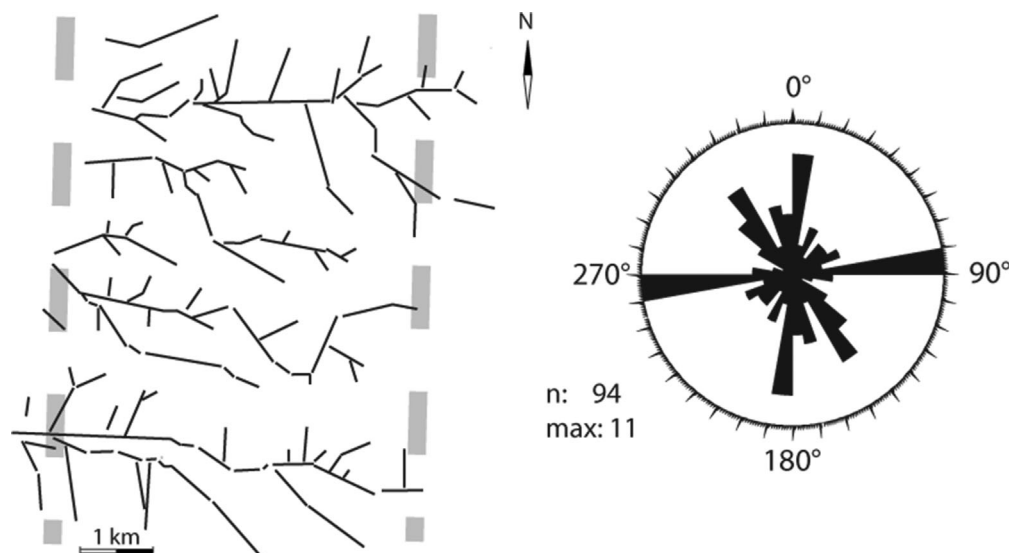


**Figure 5.** Statistical analysis of the rectified streambed directions (see text for explanation).



sectors of Rome (Marra, 2001, and references therein), where conjugated systems of ca. N60° and N120° faults, and N90° orientated fractures are observed, associated with the main N–S lineaments south of the Sabina Fault zone (Faccenna *et al.*, 1994) (Fig. 1a). In the Cretone Basin, maximum concentrations along the E–W and N–S directions are superimposed on a third maximum matching the NW–SE orientation of the major apenninic extensional faults (Fig. 5). These structural lineaments control the geometry of the depression, which probably originated because of the volcano-tectonic activity occurring in this region (Fig. 3). This activity was characterized by two principal pulses of uplift around 800 and 600 ka, coincident with the start of the main eruptive phases at the Monti Sabatini and Colli Albani Districts, and by a later uplift of ca. 40 m after 250 ka (Karner *et al.*, 2001a).

Geomorphological analysis of the basin revealed the presence of four orders of terraced depositional units, whose elevations, decreasing from east to west (i.e. towards the present alluvial plain of the Tiber River) are 80–89, 70–75, 60–65 and 50–59 m a.s.l., respectively (Fig. 3). A further surface, with subdued morphological expressions and culmination at around 105 m a.s.l., can be recognized in the easternmost portion of the basin. In light of the documented interplay between sedimentary and morphological processes and glacio-eustasy in this region (Karner *et al.*, 2001a), we interpret these terraces as remnants of alluvial plain surfaces of the Tiber River, formed during different highstands of sea level related to the Pleistocene glacio-eustatic oscillations, and successively raised to different elevation by tectonic uplift, which acted at a variable rate in the region (Karner *et al.*, 2001a; Ferranti *et al.*, 2006).

### Palaeontological data

On the whole, the recovered taxa (Table 2) indicate a wide biochronological range for the mammal assemblages collected in the different localities (Fig. 6), which can be referred to at least two distinct Mammal Ages (MA): the Galerian MA and the Aurelian MA. The palaeontological record includes the Isernia Faunal Unit (FU) and Fontana Ranuccio FU (MIS 16–15 to 12–11, Marra *et al.*, 2014a) and the Torre in Pietra and Vitinia FUs (MIS 10–9 to 8–7, Marra *et al.*, 2014a), with several species occurring also during the Late Pleistocene (Fig. 2).

Therefore, the biochronological interval of several of these taxa (those reported in bold in Table 2) provides discriminating age constraints to the lacustrine deposits in which they occur.

In particular, the Italian occurrences of *Hippopotamus antiquus*, *Axis eurygonos* and *Cervus elaphus eostephanoceros* are limited to the Galerian, with the first one not surviving after MIS 15; by contrast, *Canis lupus* and *Ursus spelaeus* appear only since MIS 9, and *Equus hydruntinus* since MIS 8.5 (Marra *et al.*, 2014a, and references therein).

*Hippopotamus antiquus* has been found in several Early and early Middle Pleistocene localities of Italy; the species became rare during the second half of the Middle Pleistocene (Petronio *et al.*, 2011) and it was replaced by *H. amphibius* after MIS 12–11 (Fig. 2) (Gliozzi *et al.*, 1997). Nevertheless, the latest Middle Pleistocene Italian records of hippopotamus are represented by very scarce and fragmentary remains that can be barely ascribed to *H. antiquus* or *H. amphibius*. Moreover, the exact stratigraphic position of the skull of *H. amphibius* collected at Tor di Quinto (see Kotsakis and Barisone, 2008, and references therein) is quite ambiguous. For these reasons, the last records of *H. antiquus* are here considered limited to MIS 15 or 13 (Marra *et al.*, 2014a).

*Axis eurygonos* occurred for the first time during the Late Villafranchian (Farneta FU) and it disappeared during the Late Galerian (Fontana Ranuccio FU, MIS 11, Fig. 2) (Petronio *et al.*, 2011). According to Di Stefano and Petronio (2002) the genus *Axis* spread at first in the Italian Peninsula and later in Continental Europe (the late Early Pleistocene *Cervus nestii vallonnetensis* is synonymous with *A. eurygonos*). The *Dama*-like cervids disappeared in Europe during the end of the Early Pleistocene (Moullé *et al.*, 2006; van der Made, 2011). The persistence of this taxon in Italy could be related to the presence of favourable climatic conditions and the role of refugia for interglacial faunas (Petronio *et al.*, 2011).

Several remains of *Cervus elaphus eostephanoceros* were collected at Osteria Moricone. This subspecies was considered as a typical taxon of the Fontana Ranuccio FU (Di Stefano and Petronio, 1993). The occurrence of *C. elaphus eostephanoceros* has been recently extended back to ca. 500 ka (MIS 13, Fig. 2; Marra *et al.*, 2014a).

*Bos primigenius* occurred early in Italy at Venosa-Notarchirico, ca. 600 ka (Cassoli *et al.*, 1999; Lefèvre *et al.*, 2010), and it was recorded together with *Bison schoetensacki*. The auroch has been recorded in the fossiliferous localities of the Roman area geochronologically dated to ca. 500 ka (Valle Giulia Formation, MIS 13, Fig. 2; Marra *et al.*, 2014a). The early aurochs appear smaller and more slender than those from the late Middle Pleistocene (Pandolfi *et al.*, 2011) and they probably originated from African species of the genus *Bos* (see Martínez-Navarro *et al.*, 2014). The parallel diffusion of *Bos* and the Acheulean culture (Mode II tools) has been established by Martínez-Navarro *et al.* (2010).

Billia and Petronio (2009) reported the first occurrence of *Stephanorhinus kirchbergensis* in Italy during the Isernia FU, at the site of Ponte Milvio. However, the specimens described by Billia and Petronio (2009), and recently revised by Pandolfi (2013), lack any stratigraphic information on the labels and display morphological features closer to *S. hundsheimensis*. Pandolfi and Marra (2015) recently reported the first occurrence of *S. kirchbergensis* at ca. 560–500 ka. *S. kirchbergensis* is well testified in the Italian Peninsula during the second half of the Middle Pleistocene and it is recorded in several sites of the area of Rome (Pandolfi and Marra, 2015, and references therein). *S. kirchbergensis* has never been recorded from Late Pleistocene Italian localities and several records attributed in the past to this species (or *Dicerorhinus mercki*) are referred to *S. hemitoechus* or *Coelodonta antiquitatis* (Pandolfi and Tagliacozzo, 2015, and references therein).

The first occurrence of *C. lupus* in Italy was chronologically related to the Torre in the Pietra FU (MIS 9, Fig. 2), as well as that of *U. spelaeus* and *Megaloceros giganteus* (Gliozzi *et al.*, 1997; Petronio *et al.*, 2011; Marra *et al.*, 2014a).

A late Middle or Late Pleistocene age is provided by *Equus hydruntinus*, which was first recorded in Italy from the 'upper gravels' of Sedia del Diavolo (Rome) (Caloi *et al.*, 1980), recently correlated to MIS 8.5 (ca. 285 ka, Marra *et al.*, 2014a, Fig. 2). However, this species was more common during the Late Pleistocene and became extinct in Italy during the Early Holocene (Petronio *et al.*, 2011).

### Palaethnological data

Abundant prehistoric lithic artefacts are associated with vertebrate fossils in the Cretone Basin (Fig. 1b). The lithic industry is generically referable to the lower Palaeolithic, consistent with that already recovered in some 20 sites in the area (Ceruleo and Zei, 1996, and references therein). The surface materials emerge in light-coloured, clayey deposits

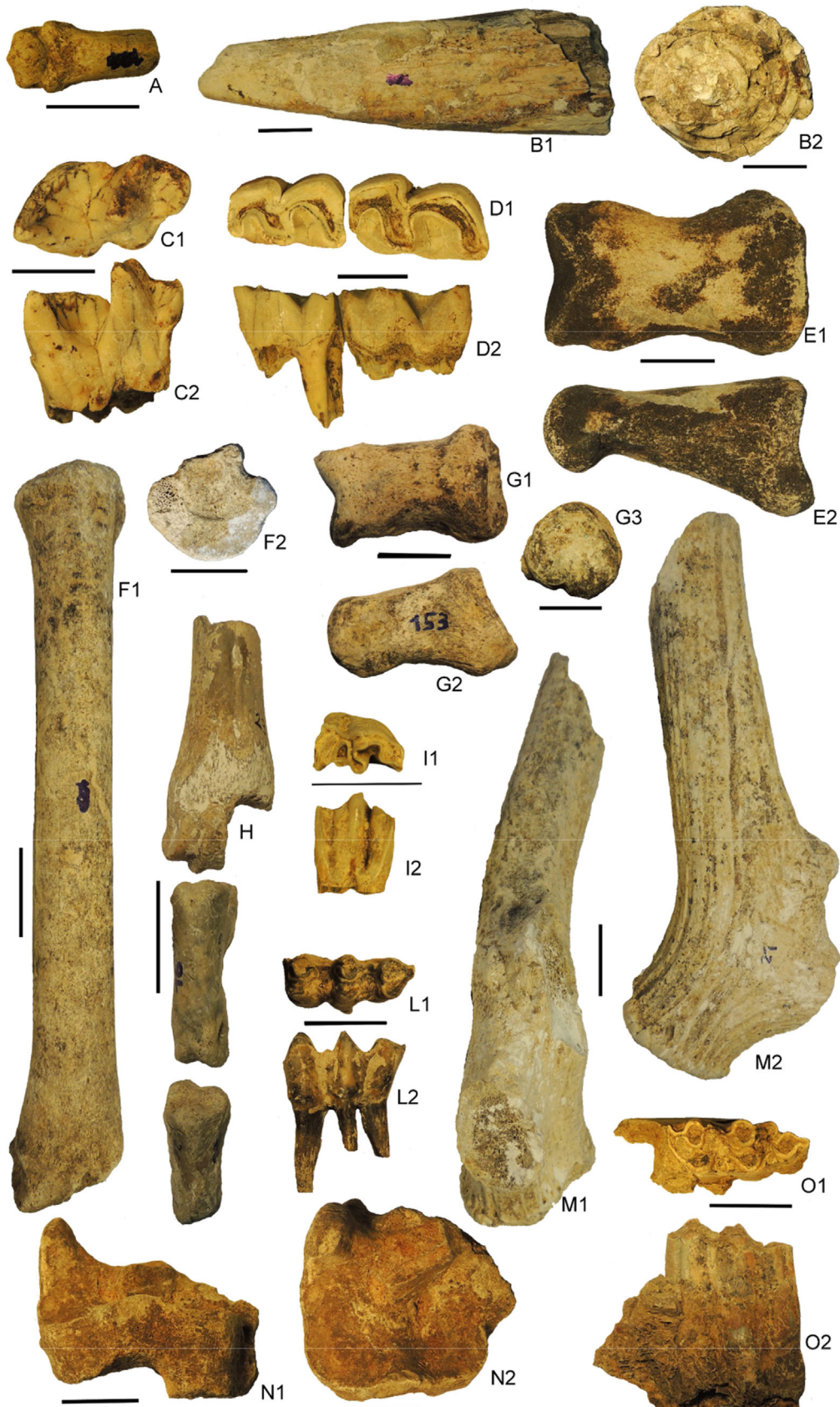


**Figure 6.** A, fragmentary metapodial bone of *Crocuta crocuta*, dorsal view; B, tusk fragment of *Palaeoloxodon antiquus*, 1 lateral view, 2 cross-section view; C, third lower molar of *Stephanorhinus cf. kirchbergensis*, 1 occlusal view, 2 lingual view; D, third and fourth lower premolars of *Stephanorhinus kirchbergensis*, 1 occlusal view, 2 lingual view; E, first phalanx of *Equus ferus*, 1 dorsal view, 2 lateral view; F, third metatarsal of *Equus hydruntinus*, 1 anterior view, 2 proximal view; G, lateral phalanx of *Hippopotamus cf. antiquus*, 1 dorsal view, 2 lateral view, 3 posterior articular view; H, metacarpal bone of *Axis eurygonos* with articulated first and second phalanges in anterior view; I, fourth lower premolar of *Cervus elaphus* ssp., 1 occlusal view, 2 labial view; L, fourth lower deciduous of *Bos vel Bison*, 1 occlusal view, 2 labial view; M, fragmentary antler of *Cervus elaphus eostephanoceros*, 1 anterior view, 2 lateral view; N, central tarsal bone of *Bison cf. schoetensacki*, 1 anterior view, 2 proximal view; O, third lower molar of *Bos primigenius*, 1 occlusal view, 2 labial view. Scale bar = 2 cm.

rich in reworked pyroclastic material and palaeosols along the flanks of the hills, which alternate with darker strata without lithic finds (Fig. 4a). A detailed description of the lithic industry is provided in a dedicated paper (Ceruleo *et al.*, 2015).

The overall homogeneity of the findings reveals substantial exploitation of raw materials even though the rudimentary typology does not match standardized characters and is possibly determined by extemporary functional needs. However, two groups of sites, corresponding to two different ‘facies’, can be recognized, based on the typological and technological features of the artefacts, together with the presence or absence of bifacials. The occurrence of bifacials may not attest to the presence of different cultural or technological contexts but instead reflects different functional usages (see Villa, 2001), as evidenced in several lower Palaeolithic sites (e.g. Notarchirico – Venosa, Piperno, 1992). In fact, in some sites of the Cretone Basin (e.g. Camporiocchio, Osteria Moricone) the bifacials constitute an important element and are concentrated in confined areas together with a relatively poor ‘accompanying’ flake industry. The first facies is richer in both stone and bone materials. The lithic industry is represented by cores, rare choppers, proto-bifaces, bifaces sometimes abundant, tools on flakes and pebbles, bone artefacts, not retouched flakes and blanks. There is a high percentage of tools compared to the total number of items and in some places there is a high percentage of bifaces. The raw material is mainly flint,

normally in the form of pebbles and, much more rarely, by carbonate rock. The physical state of the artefacts is variable: the vast majority appear without patina while others have different degrees of patina, and some are weathered because of their probable displacement. Bones are very abundant and concentrated in restricted areas mixed with stone artefacts, suggesting their likely contemporary deposition. In addition, the presence of bone artefacts, including some bifacials, with the presence of identical concretions both on stone and on bone materials favours the hypothesis that a contextual deposition occurred because of prehistoric humans.

The features described are typical of the Acheulean sites of this region, as evidenced by the presence of bone artefacts in Acheulean levels in other sites of Latium such as Anagni-Fontana Ranuccio, Colle Avarone (Ceprano), Cava Panzini (Pontecorvo), Polledrara di Ceganibbio, Malagrotta and Castel di Guido (Biddittu and Segre, 1982), Quarto delle Cintonare, Le Ferriere (ancient Satricum) and Valloncello (La Rosa *et al.*, 1992, 1996).

In contrast, the second facies, besides the absence of bifacials that may not necessarily have a chronological significance, is poorer in lithic materials and lacks bone artefacts. The lithic collection is composed primarily of flake and pebble artefacts characterized by Levallois or bipolar technique, with prepared talons and embriacted Quina or 1/2 Quina retouch, that can be referred to an early Middle Palaeolithic facies, foreboding aspects of the Mousterian (‘pre-Mousterian’; Piperno, 1992).

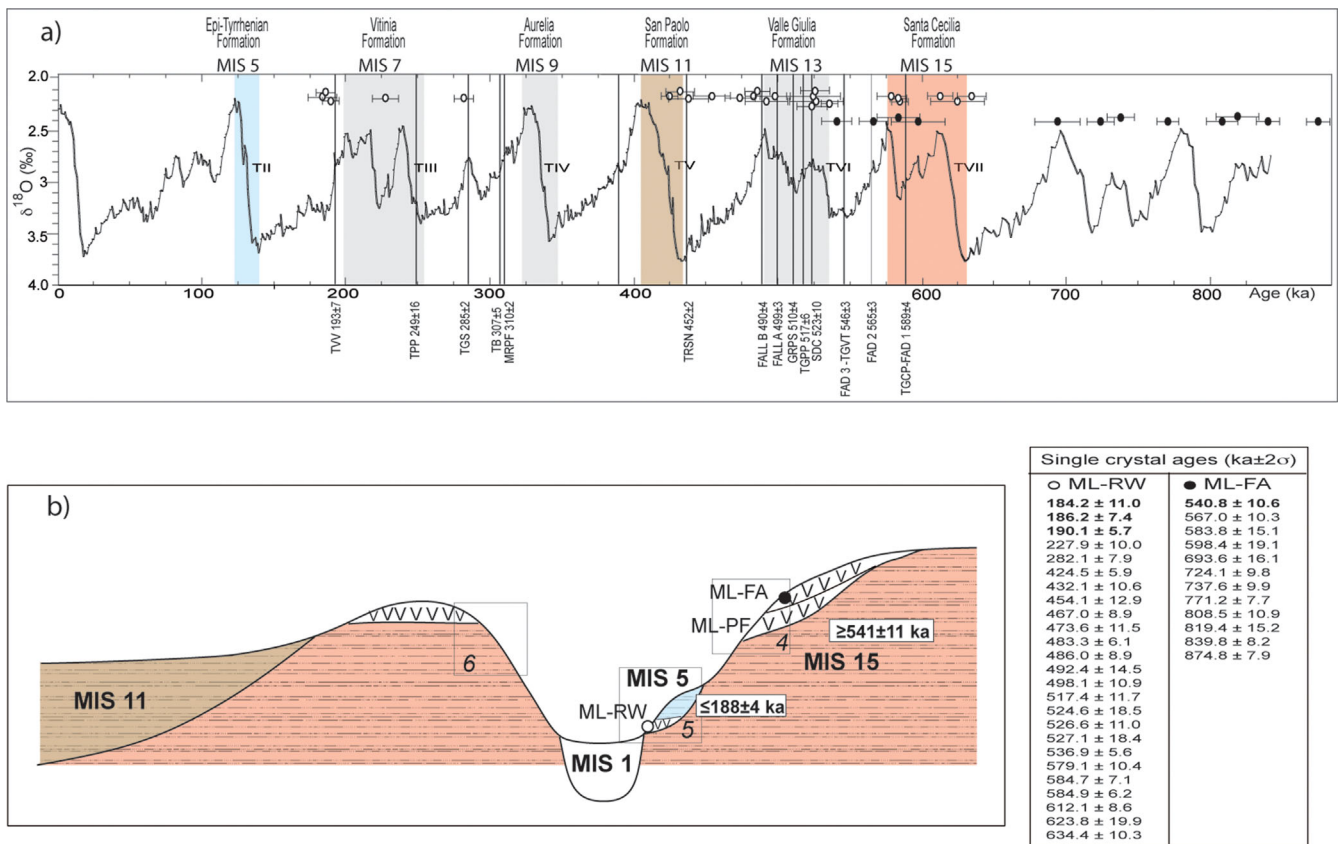


**Figure 7.** Single crystal age distributions for the two dated samples (ML-FA, ML-RW) compared to the oxygen isotopes timescale and to the eruptive history of the Monti Sabatini district (a). The vertical lines represent ages of the explosive eruptive cycles that occurred in the period 600–150 ka (Sottili *et al.*, 2010; Marra *et al.*, 2014b), with: TGCP, Tufo Giallo di Castelnuovo di Porto; FAD, First Ashfall Deposits; TGVV, Tufo Giallo della via Tiberina; SDC, Sella di Corno; TGPP, Tufo Giallo di Prima Porta; GRPS, Grottarossa Pyroclastic Sequence; TRSN, Tufo Rosso a Scorie Nere; SAAS, San Abbondio Ashfall Succession; MRPF, Magliano Romano Plinian Fall; TB, Tufo di Bracciano; TGS, Tufo Giallo di Sacrofano; TPP, Tufo di Pizzo Prato; TVV, Tufo di Vigna di Valle. The shaded portion of the curve represent the sedimentary cycles associated with periods of sea-level rise during glacial terminations. (b) Chronostratigraphic setting and inferred age of deposition for the different lacustrine successions in which the dated samples are intercalated.



## Geochronological and geochemical data

### $^{40}\text{Ar}/^{39}\text{Ar}$ ages

#### Sample ML-FA

Twelve sanidine crystals from sample ML-FA yielded scattered ages ranging from  $875 \pm 8$  to  $541 \pm 11$  ka, confirming the strongly reworked origin of the deposit (Fig. 7a; Supplementary online material 1). However, the four youngest crystal ages ( $598 \pm 19$ ,  $584 \pm 15$ ,  $567 \pm 10$ ,  $541 \pm 11$  ka) match those of the three FAD units (Monti Sabatini First Ashfall Deposits), dated to  $589 \pm 4$ ,  $565 \pm 3$  and  $546 \pm 5$  ka (Karner *et al.*, 2001b; Marra *et al.*, 2014b, Fig. 7a). The lack of crystals younger than 541 ka in the deposit is an indication that the age of emplacement is not much younger. Indeed, younger Plinian fallout and pyroclastic deposits from widespread Monti Sabatini eruptions top the lacustrine succession in other sectors of the Cretone Basin [i.e. Fall A and Tufo Giallo di Prima Porta (TGPP):  $499 \pm 3$  and  $517 \pm 6$  ka, respectively; Sottili *et al.*, 2004; Marra *et al.*, 2014b; see below]. We suggest that the lack of crystals from Fall A and TGPP confirm the hypothesis that the sediment containing ML-FA was deposited before these eruptions. We therefore interpret the underlying massive pyroclastic deposit (ML-PF in Fig. 7b), in which feldspar is missing and abundant biotite occurs, as a distal facies of the widespread Tufo Giallo della Via Tiberina eruption (TGVT;  $546 \pm 3$  ka; Marra *et al.*, 2014b, Fig. 7a), whereas the upper, granular pyroclastic layer from which ML-FA was collected may represent a reworked deposit, containing a concentrated fraction of older volcanics intercalated in the lacustrine succession and overlying older deposits on the morphological highs, eroded and re-deposited during the regressive phase between the end of MIS 15 (580 ka) and beginning of MIS 14 (535 ka).

#### Sample ML-RW

Twenty-five sanidine crystals from sample ML-RW yielded scattered ages ranging from  $634 \pm 10$  to  $184 \pm 11$  ka, highlighting also in this case the reworked origin of these volcanoclastic deposits (Fig. 7a; Supplementary Online Material 1). However, the three youngest crystals yield a weighted mean age of  $188 \pm 4$  ka, indicating that the lacustrine succession at the base of which ML-RW occurs is younger than the deposits containing the faunal assemblage described by Manni *et al.* (2000), for which an age of  $\geq 541$  ka is inferred (Fig. 7b).

The 184 ka age is consistent with that of the regressive phase following MIS 7 (Fig. 7a). The occurrence of this volcanoclastic layer within the coarse-grained, basal portion of the lacustrine deposit is consistent with the hypothesis of a strict link between glacio-eustatic fluctuations and sedimentation in this region, suggesting that this succession was deposited during the penultimate glacial termination, in response to sea-level rise during MIS 5 (Fig. 7).

### Geochemical analyses

#### Sample ML-FAD

Both Zr/Y vs. Nb/Y and Zr/TiO<sub>2</sub> vs. Nb/TiO<sub>2</sub> of sample ML-FAD (Fig. 8a–a'), combined with its depositional feature, allow us to correlate with the fallout deposit of FAD 1 dated to  $589 \pm 4$  ka (Marra *et al.*, 2014b).

#### Sample ML-Fall A

The lithological and textural features of this pumice fallout deposit match strictly those of the Lower Fall A1 layer, a widespread and diagnostic marker fallout (Sottili *et al.*, 2004)

as part of the Tufi Terrosi *con* Pomici Bianche pumice and scoria-fall succession (Karner *et al.*, 2001b). Particularly relevant is the presence in ML-Fall A of millimetre-sized, thermally metamorphosed reddish lithics, which is a diagnostic characteristic of the Plinian Fall A unit (Sottili *et al.*, 2004) even in distal settings (e.g. Giaccio *et al.*, 2014). The Zr/Y vs. Nb/Y composition of sample ML-Fall A (Fig. 8a–a') confirms attribution to the lower Fall A1 unit, for which an age of  $\geq 499 \pm 3$  ka (upper Fall A1) and  $< 510 \pm 9$  ka (Grottarossa Pyroclastic Sequence, GRPS) is inferred from the Cava Rinaldi chronostratigraphy (Marra *et al.*, 2014b).

#### Sample ML-TG

The trace-element composition of this sample, plotting in the lower portion of the Zr/Y vs. Nb/Y and Zr/TiO<sub>2</sub> vs. Nb/TiO<sub>2</sub> diagrams (Fig. 8b–b'), suggests a poorly evolved chemistry which, among the Monti Sabatini 'tufi gialli', finds correspondence only in the TGPP pyroclastic-flow deposit (Marra *et al.*, 2014b). Correlation of the pyroclastic-flow deposit from which sample ML-TG was collected to the  $517 \pm 6$  ka TGPP (Marra *et al.*, 2014b) is also supported by its stratigraphic position below Fall A (Fig. 9) and by the dispersal area of the TGPP as described by Marra *et al.* (2014b).

#### Sample ML-RL

The trace-element composition of this deeply reworked sample should be considered as merely indicative of its possible provenance. However, its position in the lowest part of both diagrams (Fig. 8b–b') matches the composition of the least differentiated products of the Sabatini Volcanic District, which is distinctive of the GRPS ( $511 \pm 9$  ka, Marra *et al.*, 2014b). This pyroclastic-flow deposit was emplaced soon after glacial termination V, at the onset of MIS 13 (Fig. 2), suggesting that the lacustrine deposit in which sample ML-RL was collected correlates with this isotopic stage.

## Discussion

### Evolution of the Cretone Basin

#### Sedimentary, palaeontological and palaeoethnological implications

We have correlated each of the four orders of terraces recognized through the morpho-structural analysis with odd-numbered marine isotopic stages, following the conservative principle of assigning a progressive MIS number starting from the present-day alluvial plain of the Tiber River, which matches MIS 1 (see cross-section A–B of Fig. 3). The elevations of four MIS-related Cretone terraces are consistent with those that have been correlated, using geochronological constraints, to the different odd marine isotopic stages in the coastal area of Rome and in the ancient delta of the Tiber River (Fosso Galeria area) (Fig. 3; Marra *et al.*, 2014a, 2015b, and references therein). In particular, the relative elevations of the terraces within the Cretone Basin are consistent with the occurrence of a late uplift pulse of approximately 45 m since 250 ka, which accounts for the large difference in elevation between MIS 1 and MIS 7 (ca. 235 ka), and for the fact that the MIS 5 (ca. 125 ka) terrace (surface d in Fig. 3) should be at lower elevation with respect to that of MIS 7 (surface c in Fig. 3), despite the higher sea level reached during this younger isotopic event.

The uplift pulse since 250 ka was preceded by a substantial stasis between 500 and 250 ka (Karner *et al.*, 2001a), as also inferred from the small differences in altitude among MIS 11 (ca. 410 ka), MIS 9 (ca. 330 ka) and MIS 7, reflecting the

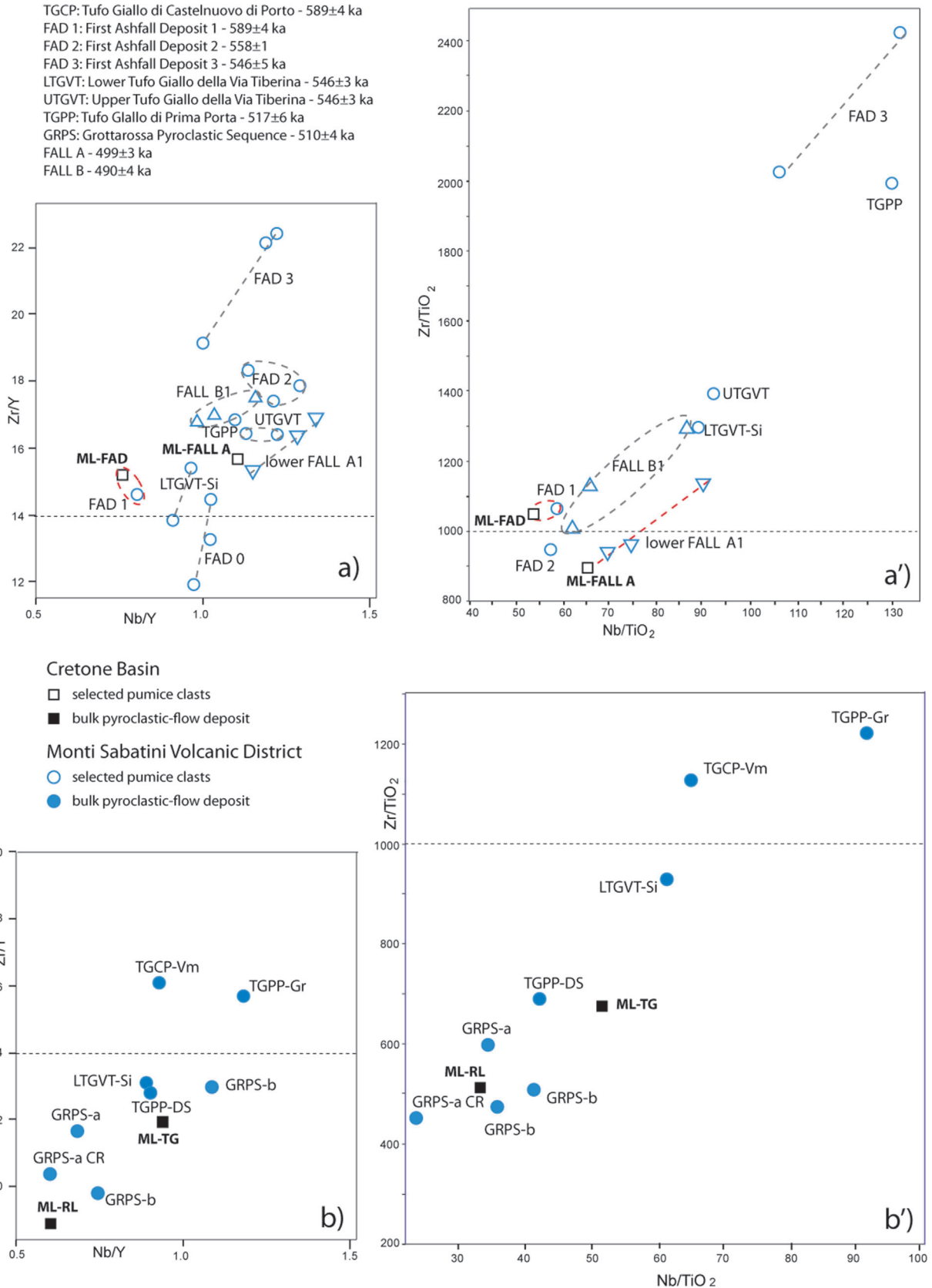


**Figure 8.** Classification diagrams comparing selected trace-element compositions of the analysed samples to those of the products of the Monti Sabatini volcanic district. Samples ML-FAD and ML-FALL A plot in the upper portion (above the dashed horizontal lines) of the Zr/Y vs. Nb/Y and Zr/TiO<sub>2</sub> vs Nb/TiO<sub>2</sub> diagrams (a and a'), and their compositions match those of FAD-1 and lower Fall A1, respectively, based on criteria established by Marra *et al.* (2014b) and Marra *et al.* (2015b). Samples ML-TG and ML-LR display lower ratios (below the dashed lines) in both diagrams (b and b'), and are attributed to Tufo Giallo di Prima Porta and Grottarossa Pyroclastic Sequence, respectively. In particular, the combined use of the two diagrams provides a best fit for each sample based on similar composition as well as consistent linear trend (when defined) with respect to the reference rock samples (Marra *et al.*, 2014b, and references therein).

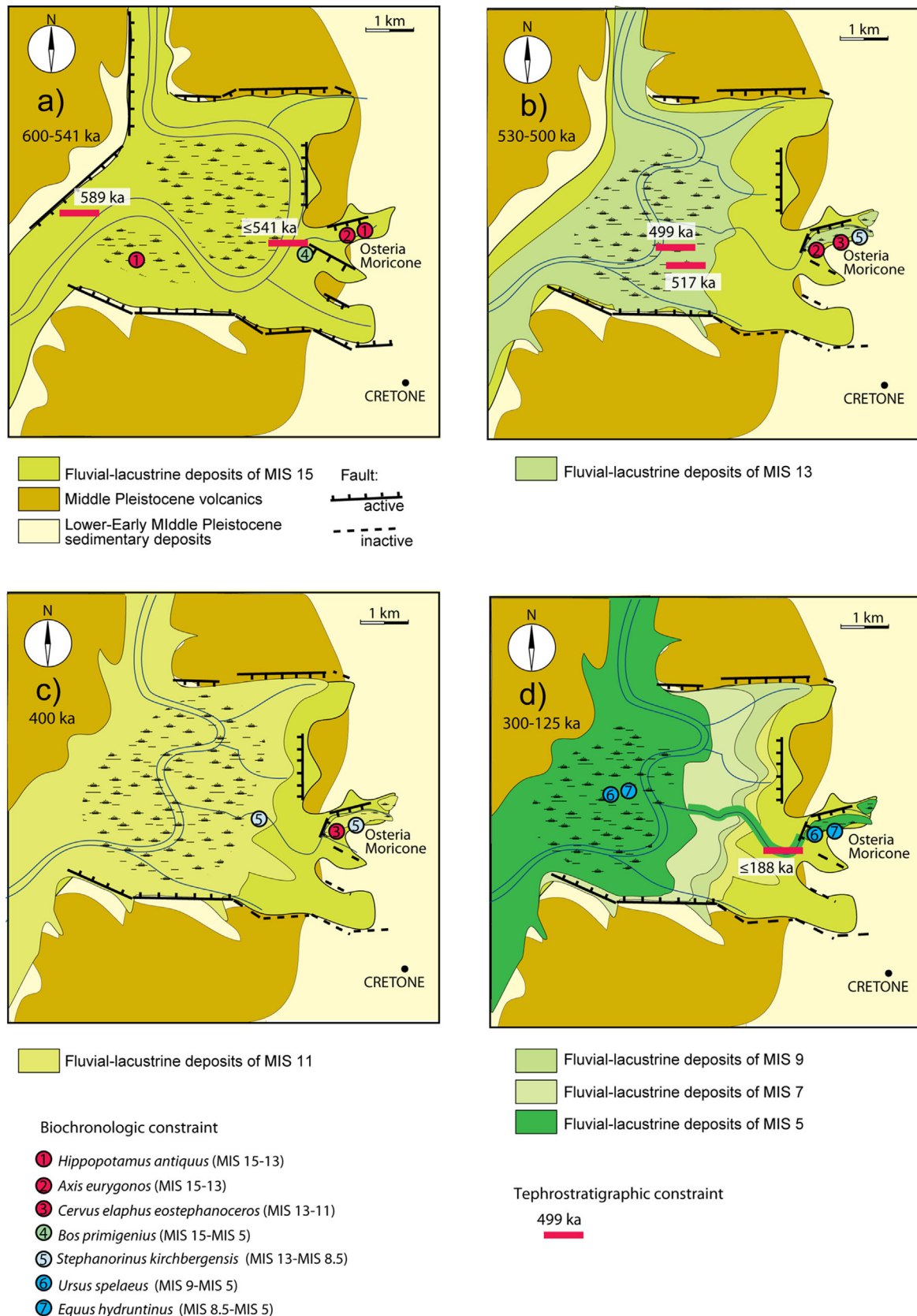


**Figure 9.** Geological evolution of the Cretone Basin according to the biostratigraphic and tephrostratigraphic constraints provided in this study. The chronological range for the reported taxa refers to the time span 600–125 ka and is indicated by the encompassed marine isotope stages, to provide biochronological constraints to the lacustrine deposits. (a) Initial stages of formation of the lacustrine basin during late MIS 15 as a consequence of the 600 ka extensional phase, re-activating pre-existing fault segments. (b) Westward migration and size reduction of the basin as a consequence of intervening uplift and the lower sea level during MIS 13, accompanied by the origin of a satellite basin in Osteria Moricone. (c) A larger lake occupies the Cretone Basin around 400 ka, due to the higher sea level during MIS 11. (d) Continued regional uplift causes the further westward migration of the basin and the origin of a series of terraced surfaces correlating with MIS 9–5.





lacustrine basin in the late stages of MIS 15 (Fig. 9a), consistent with the occurrence of an extensional tectonic phase associated with the start of the explosive activity at Colli Albani and Monti Sabatini volcanic districts (Marra and Florindo, 2014). Because of regional uplift of ca. 20 m after 600 ka (Karner *et al.*, 2001a), the deposits attributed to MIS 15 in the eastern portion of the Cretone Basin occur at higher elevation with respect to those of the following glacio-eustatically controlled sedimentary cycles (Fig. 10). For example, the relic surface attributed to the MIS 15 terrace has a top elevation around 105 m a.s.l. compared to that of about 85 m a.s.l. for the MIS 11 terrace (Figs 10 and 11).

The occurrence of the pyroclastic-flow deposit of TGPP (517 ± 4 ka) and of the Plinian Fall A deposit (499 ± 3 ka) within the lacustrine succession found around 70 m a.s.l. in the western portion of the basin (Section 3; Fig. 10) suggests continued sedimentation during MIS 13, yet occurring at lower elevation with respect to the previous glacio-eustatic cycle of MIS 15, in agreement with uplift of this area and the consequent decreasing dimension and westward migration of the basin (Fig. 9b). Moreover, the occurrence of a faintly pedogenized sedimentary deposit above the Fall A deposit (Section 3), covered by more lacustrine deposits, suggests a sedimentary hiatus was followed by younger aggradation. This is consistent with continued filling of the fluvial-lacustrine basin during the subsequent glacio-eustatic cycle up to the terraced surface at around 85 m a.s.l. that correlates to the highstand of MIS 11 (T11, see also detailed morpho-structural map in Supplementary Online material 5). Regional and global evidence exists favouring a markedly high sea level at ca. 400 ka during MIS 11 (Karner and Marra, 2003). The terrace formed during MIS 13 was drowned during MIS 11, the highest terrace in the western portion of the basin (Figs 9c and 10). Therefore, all the deposits occurring above this elevation in the eastern portion of the basin should be considered uplifted and older, not only than 400 ka, but also than 500 ka, because of lower elevation of the MIS 13 terrace,

and thus are correlated to MIS 15 (Supplementary Online material 5).

Nevertheless, the lithic industry recovered in Osteria Moricone is characterized by the presence of two apparently distinct technological, typological features that can be ascribed to an early Acheulean age (older than 300 ka) and to a later early Middle Pleistocene age (Ceruleo *et al.*, 2015). Similarly, the palaeontological record recovered in this small area, which includes species that appear only since MIS 9 (*Ursus spelaeus*) and since MIS 8.5 (*Equus hydruntinus*), along with others spanning MIS 15–11, provides evidence of sedimentation well after 400 ka in this restricted sector (Figs 9d, 10 and 11). This is probably the consequence of the volcano-tectonic phase occurring after 600 ka, responsible for the uplift and erosion of the MIS 15 terrace, leaving only small relics of its depositional surface (T15, see also Supplementary Online material 5) with the re-activation of fault segments controlling the present-day course of the Moricone streambed in this sector. This may have generated a small tectonic basin in which lacustrine sedimentation persisted through MIS 13–5 (Fig. 9b–d).

The fossil remains of *Cervus elaphus eastephanoceros*, *Bos primigenius*, *Stephanorhinus kirchbergensis* and *Equus hydruntinus*, along with the Acheulean and pre-Mousterian lithic industry, were probably embedded within the sediments of this small lake after MIS 13, which would have represented an attractive area for a large number of herbivorous animals and for their hunters or scavengers, including *Homo*, until MIS 5.

In the same time period, a larger fluvial-lacustrine basin was developed in the western portion of the area, corresponding to the ancient alluvial plain of the Tiber River, where the terraces of the corresponding glacio-eustatic cycles of MIS 11, 9, 7 and 5 are preserved, although partially eroded because of the uplift phase occurring since 250 ka. The presence of *Hippopotamus cf. antiquus* and *Ursus cf. spelaeus* remains in the lower western portion of the basin

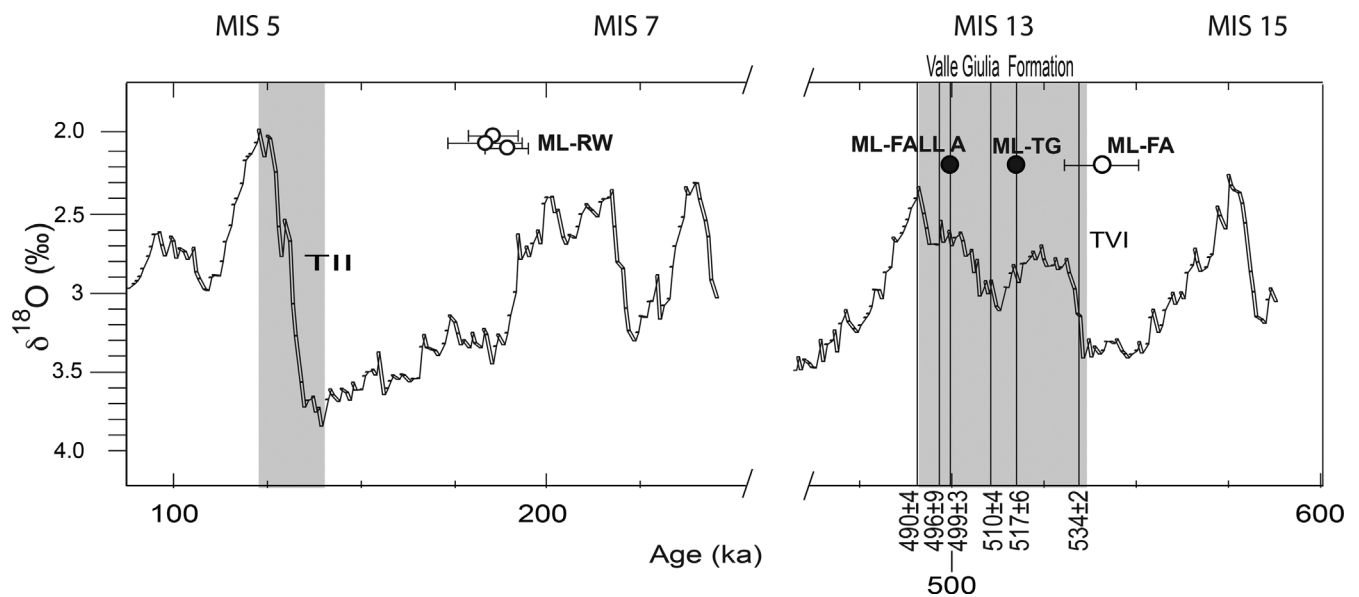


**Figure 11.** Geochronological constraints to the sedimentary cycles occurring in the Cretone Basin, represented by volcanic deposits dated for the present study (samples ML-FA, ML-RW) or correlated to the eruptive cycles of the Monti Sabatini Volcanic District dated by Marra *et al.* (2014b) (samples ML-TG = TGPP, ML-FALL A = Fall A1), are compared to those achieved by previous studies (Marra *et al.*, 2008, and references therein) on the sedimentary successions of the area of Rome (vertical lines). The open circle represents a *post quem* for initiation of Glacial Termination VI, whereas full circles represent phases of aggradation after the terminations. There is a very good match between phases of aggradation within the Cretone Basin and those occurring near the Tyrrhenian Sea coast, together with a strict coupling with the sea-level rise during MIS 13. Youngest ages of sample ML-RW provide a *post quem* for Glacial Termination II, and represent the first geochronological constraint achieved for this glacio-eustatic event in this region.

(Figs 9a,c and 10), combined with the attribution to MIS 13 of the lacustrine deposit of Section 2, supports the occurrence of a long stratigraphic record, spanning MIS 15–7, at the least. However, the largest volume of the sedimentary filling of the basin probably spans MIS 15–13, whereas the MIS 11–5 deposits are confined within the fluvial incisions or form small remnants of terraced surfaces and are represented by thin successions of fluvial–palustrine deposits and pedogenetic horizons. A remnant of the aggradational succession deposited during MIS 5 sea-level rise is found within the Moricone stream valley (Figs 9d, 10 and 11), where their base level is higher than that of the present-day alluvial deposits because of the last pulse of uplift. This base level is represented by the closely dashed line in the cross-section of Fig. 10, connecting to that inferred for the terraced deposits of MIS 5. The corresponding terraced surfaces occur around 55 m a.s.l., and ca. 30 m above the present-day alluvial plain of the modern Tiber River, consistent with elevation of the coastal terrace of MIS 5 spanning 35–40 m a.s.l. (Marra *et al.*, 2015a).

The continued regional uplift during MIS 5 caused the extinction of the lacustrine basin of Cretone, as well as of the smaller lake in Osteria Moricone, due to the erosion of its threshold.

### Implications for glacio-eustatic oscillations

Ages of the volcanic deposits intercalated within the lacustrine succession of the Cretone Basin provide evidence of the strict link between glacio-eustatic-driven sea-level rise during glacial terminations and sedimentary cycles in this sector of the Tiber River hydrographic basin, and are consistent with observations in the coastal area of this region (Marra *et al.*, 2008, and references therein). In particular, the new data presented in this paper constrain aggradation during sea-level rise of MIS 13, providing an age of  $<541 \pm 10$  ka for the late regressive phase of MIS 14, an age of  $>517 \pm 6$  for glacial termination VI, and an age of  $\geq 499 \pm 3$  ka for the highstand of MIS 13 (Fig. 11). These data are in good agreement with those provided for the aggradational succession deposited during MIS 13 in the coastal area (Cava Rinaldi section) and within the city of Rome (Valle Giulia Formation; Karner and Marra, 1998; Marra *et al.*, 2014b), demonstrating the strong glacio-eustatic forcing on the sedimentary history in this sector of the Tyrrhenian Sea margin.

Moreover, the age of  $188 \pm 4$  ka (sample ML-RW) provided here to the regressive phase of MIS 7 gives a *post quem* for aggradation during sea-level rise of MIS 5 (Fig. 11), and represents the first geochronological constraint achieved so far in the area of Rome for the penultimate glacial termination.

### Concluding remarks

Our results, within the framework provided in previous studies for this sector of the Tyrrhenian Sea margin of Italy, indicate that the depositional phases within the lacustrine basin of Cretone were influenced strongly by glacio-eustatic cyclicity, despite its distance of about 50 km from the present-day coastline. Evidence for this glacio-eustatic influence can be found in the synchronicity of the depositional cycles with the periods of sea-level rise during the glacial terminations. Elevation gain between the terraced surfaces of the different aggradational successions is the result of the interplay between glacio-eustatism and tectonic uplift.

Geochronological and biostratigraphic data presented in this study show that the Cretone Basin originated around

600 ka through re-activation of pre-existing fault segments, during the early stages of the regional volcano-tectonism that the region underwent before the onset of the main explosive activity at the Monti Sabatini and Colli Albani volcanic districts. In this period, *Hippopotamus*, *Palaeoloxodon antiquus* and *Bos primigenius* frequented this area and were hunted or scavenged by local Palaeolithic groups, as testified by fossil and lithic industry remains embedded in the lacustrine deposits filling this early basin during the sea-level rise of MIS 15.

Coupled extensional tectonics and volcanic deformations between 600 and 500 ka caused the uplift and westward migration of the main lacustrine basin, while a smaller lake originated at its eastern margin in Osteria Moricone. In this area, stable environmental conditions favoured continuous faunal (*Homo* included) frequentation and the preservation of fossil and lithic industry remains, as testified by the palaeontological and palaeoethnological findings, ascribable to the Aurelian Mammal Age and to pre-Mousterian industries, respectively. In contrast, the western sector was connected to the Tiber River alluvial plain and was more directly affected by erosional and depositional processes driven by sea-level fluctuations during the successive glacio-eustatic cycles. Sedimentary successions in this area occur as fluvial terraces correlated with MIS 11–5, progressively lower in elevation (ca. 85–55 m a.s.l., respectively) and overlying the tectonically lowered MIS 13 terrace. However, the oldest lacustrine deposits correlated to MIS 15 occur at higher elevation in the eastern, tectonically uplifted portion of the Cretone Basin. The attribution to MIS 15 of the deposit hosting the faunal assemblage described by Manni *et al.* (2000) allows us to make some considerations about the first occurrence of *B. primigenius* in central Italy, which was previously thought to occur during MIS 13 in the Fontana Ranuccio FU (Marra *et al.*, 2014a). Although rare, the presence at around 600 ka of *B. primigenius* in the Cretone Basin of central Italy is coincident with the early appearance of this species within the Isernia FU in the Venosa-Notarchirico locality of southern Italy. In this locality, however, *Bison schoetensacki* largely prevails over *B. primigenius*, supporting the notion that this former species initially prevented the diffusion of the latter. Finally, analogously to Venosa-Notarchirico (Martínez-Navarro *et al.*, 2007, 2010; Pandolfi *et al.*, 2011), the documented early occurrence of *B. primigenius* in the lacustrine deposit of the Cretone Basin is associated with the presence of Acheulean lithic industry, supporting the parallel diffusion of the auroch and the Acheulean culture. In particular, part of the lithic industry recovered in the Cretone Basin, dating as far back as  $\sim 550$  ka, may represent one of the oldest evidence of Acheulean culture in central Italy.

*Abbreviations.* FAD, First Ashfall Deposit; FU, Faunal Unit; GRPS, Grottarossa Pyroclastic Sequence; MA, Mammal Age; MIS, Marine Isotope Stage; TGPP, Tufo Giallo di Prima Porta.

### Supporting Material

- 1: Table S1.  $^{40}\text{Ar}/^{39}\text{Ar}$  age data for samples ML-FA and ML-RW.
- 2: Sample description.
- 3: Geochemical analyses.
- 4: Palaeontology.
- 5: Morpho-structural map showing detail of the Osteria Moricone sector in the eastern portion of the Cretone Basin.



## References

- Bidditu I, Segre AG. 1982. Utilizzazione dell'osso nel Paleolitico inferiore italiano. *Atti XXIII Riunione Scientifica IIPP Firenze*: 89–105.
- Billia EME, Petronio C. 2009. Selected records of *Stephanorhinus kirchbergensis* (Jäger 1839) (Mammalia Rhinocerotidae) in Italy. *Bollettino della Società Paleontologica Italiana* **481**: 21–32.
- Bordes F. 1961. Typologie du Paléolithique ancien et moyen. *Delmas: Bordeaux*.
- Caloi L, Palombo MR, Petronio C. 1980. La fauna quaternaria di Sedia del Diavolo (Roma). *Quaternaria* **22**: 177–209.
- Caputo C, Ciccacci S, De Rita D et al. 1993. Drainage pattern and tectonics in some volcanic areas of Latium (Italy). *Geologica Romana* **29**: 1–13.
- Cassoli PF, Di Stefano G, Tagliacozzo A. 1999. I vertebrati dei livelli superiori (A e Alfa) della serie stratigrafica di Notarchirico. In *Notarchirico un sito del Pleistocene medio-iniziale nel bacino di Venosa (Basilicata)*, Piperno M (ed.). *Osanna Venosa I*: 361–438.
- Ceruleo P, Marra F, Pandolfi L et al. 2015. The archaic Acheulean lithic industry of the Cretone basin (Latium, central Italy). *Journal of Archaeological Science: Reports* **3**: 480–492.
- Ceruleo P, Zei M. 1996. Il paleolitico inferiore di Cretone (Roma). In *The Workshops and the Posters of the XIII International Congress of Prehistoric and Protohistoric Sciences, Forl*: 244–245.
- Conato V, Esu D, Malatesta A et al. 1980. New data on the Pleistocene of Rome. *Quaternaria* **22**: 131–176.
- Di Canzio E, Bedetti C, Petronio C et al. 2003. Middle Pleistocene vertebrate fauna from Cretone (Sabina Latium). *Bollettino della Società Paleontologica Romana* **42**: 129–132.
- Di Stefano G, Petronio C. 1993. A new *Cervus elaphus* of Middle Pleistocene age. *Neues Jahrbuch für Geologie und Paläontologie – Abhandlungen* **190**: 1–18.
- Di Stefano G, Petronio C. 2002. Systematics and evolution of the Eurasian Plio-Pleistocene tribe Cervini (Artiodactyla Mammalia). *Geologica Romana* **36**: 311–334.
- Dogliani C, Gueguen E, Harabaglia P et al. 1999. On the origin of west-directed subduction zones and applications to the western Mediterranean. In Durand B, Jolivet L, Horvath F, Seranne F (eds). Geological Society: London, 541–561.
- Faccenna C, Funicello R, Mattei M. 1994. Late Pleistocene N-S shear zones along the Latium Tyrrhenian margin: structural characters and volcanological implications. *Bollettino di Geofisica Teorica Applicata* **36**: 507–522.
- Ferranti L, Antonioli F, Mauz B et al. 2006. Markers of the last interglacial sea-level high stand along the coast of Italy: tectonic implications. *Quaternary International* **145–146**: 30–54.
- Florindo F, Karner D, Marra F et al. 2007. Radioisotopic age constraints for glacial terminations IX and VII from aggradational sections of the Tiber River delta in Rome, Italy. *Earth and Planetary Science Letters* **256**: 61–80.
- Giaccio B, Galli P, Peronace E et al. 2014. A 560–440 ka tephra record from the Mercure Basin, southern Italy: volcanological and tephrostratigraphic implications. *Journal of Quaternary Science* **29**: 232–248.
- Girrotti O, Mancini M. 2003. Plio-Pleistocene stratigraphy and relations between marine and non-marine successions in the middle valley of the Tiber River (Latium Umbria). *Il Quaternario* **16**: 89–106.
- Gliozzi E, Abbazzi L, Ambrosetti PG et al. 1997. Biochronology of selected mammals molluscs and ostracods from the Middle Pliocene to the Late Pleistocene in Italy – the state of the art. *Rivista Italiana di Paleontologia e Stratigrafia* **103**: 369–388.
- Jicha BR, Singer BS, Sobol P. 2016. Re-evaluation of the ages of  $^{40}\text{Ar}/^{39}\text{Ar}$  sanidine standards and supereruptions in the western U.S. using a Noblesse multi-collector mass spectrometer. *Chemical Geology* dx.doi.org/10.1016/j.chemgeo.2016.03.24.
- Karner DB, Marra F. 1998. Correlation of fluviodeltaic aggradational sections with glacial climate history: A revision of the Pleistocene stratigraphy of Rome. *Geological Society of America Bulletin* **110**: 748–758.
- Karner DB, Marra F. 2003.  $^{40}\text{Ar}/^{39}\text{Ar}$  dating of Glacial Termination V and duration of the Stage 11 highstand. In *Earth's Climate and Orbital Eccentricity: The Marine Isotope Stage 11 Question*. American Geophysical Union, *Geophysical Monograph* **137**: 61–66.
- Karner DB, Marra F, Florindo F et al. 2001a. Pulsed uplift estimated from terrace elevations in the coast of Rome: evidence for a new phase of volcanic activity? *Earth and Planetary Science Letters* **188**: 135–148.
- Karner DB, Marra F, Renne PR. 2001b. The history of the Monti Sabatini and Alban Hills volcanoes: groundwork for assessing volcanic-tectonic hazards for Rome. *Journal of Volcanology and Geothermal Research* **107**: 185–219.
- Kotsakis T, Barisone G. 2008. I vertebrati fossili continentali del Plio-Pleistocene dell'area romana. In *La Geologia di Roma*, Funicello R, Praturlon A, Giordano G (eds). *Memorie Descrittive della Carta Geologica d'Italia* **80**: 115–143.
- La Rosa M, Mazza P, Moggi Cecchi J et al. 1992. Late Middle Pleistocene mammal and Paleolithic remains from Campoverde Latium Central Italy. *Antropologia Contemporanea* **15**: 65–83.
- La Rosa M, Milliken S, Peretto C. 1996. Il sito del Paleolitico inferiore di Quarto delle Cianfonare (LT) Ambiente paleogeografico e sfruttamento della selce. *Atti XI Congresso degli Antropologi Italiani Isernia, Italy*: 143–154.
- Lefèvre D, Raynal JP, Vernet G et al. 2010. Tephro-stratigraphy and the age of ancient southern Italian Acheulean settlements: the sites of Loreto and Notarchirico (Venosa Basilicata Italy). *Quaternary International* **223**: 360–368.
- Lisiecki LE, Raymo ME. 2005. A Pliocene-Pleistocene stack of 57 globally distributed benthic  $\delta^{18}\text{O}$  records. *Paleoceanography* **20**: PA1003.
- Manni R, Margottini S, Palombo MR, et al. 2000. Scavo e recupero di resti di Elephas (Palaeoloxodon) antiquus Falconer & Cautley nei pressi di Palombara Sabina (Roma). *Atti del 2° Convegno Nazionale di Archeozoologia Abaco Forl*: 99–106.
- Marra F. 2001. Strike-slip faulting and block rotation: a possible triggering mechanism for lava flows in the Alban Hills? *Journal of Structural Geology* **23**: 127–141.
- Marra F, Ceruleo P, Jicha B et al. 2015a. A new age within MIS 7 for the *Homo neanderthalensis* of Saccopastore in the glacio-eustatically forced sedimentary successions of the Aniene River Valley, Rome. *Quaternary Science Reviews* **129**: 260–274.
- Marra F, D'Ambrosio E, Gaeta M et al. 2015b. Petro-chemical identification and insights on chronological employment of the volcanic aggregates used in ancient Roman mortars. *Archaeometry* in press.
- Marra F, Florindo F. 2014. The subsurface geology of Rome: sedimentary processes, sea-level changes and astronomical forcing. *Earth-Science Reviews* **136**: 1–20. DOI: 10.1016/j.earscirev.2014.05.001
- Marra F, Florindo F, Boschi E. 2008. History of glacial terminations from the Tiber River, Rome: Insights into glacial forcing mechanisms. *Paleoceanography* **23**: PA2205.
- Marra F, Florindo F, Karner DB. 1998. Paleomagnetism and geochronology of early Middle Pleistocene depositional sequences near Rome: comparison with the deep sea  $\delta^{18}\text{O}$  climate record. *Earth and Planetary Science Letters* **159**: 147–164.
- Marra F, Pandolfi L, Petronio C et al. 2014a. Reassessing the sedimentary deposits and vertebrate assemblages from Ponte Galeria area (Rome, central Italy): an archive for the Middle Pleistocene faunas of Europe. *Earth-Science Reviews* **139**: 104–122.
- Marra F, Sottili G, Gaeta M et al. 2014b. Major explosive activity in the Monti Sabatini Volcanic District (central Italy) over the 800–390 ka interval: geochronological-geochemical overview and tephrostratigraphic implications. *Quaternary Science Reviews* **94**: 74–101.
- Martínez-Navarro B, Pérez-Claros JA, Palombo MR, Rook L, Palmqvist P. 2007. The olduvai buffalo Pelorovis and the origin of Bos. *Quaternary Research* **68**: 220–226.
- Martínez-Navarro B, Rook L, Papini M et al. 2010. A new species of bull from the Early Pleistocene paleoanthropological site of Buia (Eritrea): Parallelism on the dispersal of the genus Bos and the Acheulean culture. *Quaternary International* **212**: 169–175.
- Martínez-Navarro B, Karoui-Yaakoub N, Oms O, et al. 2014. The early Middle Pleistocene archeopaleontological site of Wadi Sarrat,

- Tunisia and the earliest record of *Bos primigenius*. *Quaternary Science Reviews* **90**: 37–46.
- Milli S, Moscatelli M, Palombo MR *et al.* 2008. Incised valleys their filling and mammal fossil record A case study from middle-Upper Pleistocene deposits of the Roman Basin (Latium Italy) In *Advances in Application of Sequence Stratigraphy in Italy*, Amorosi A, Haq BU, Sabato L (eds). *GeoActa Special Publication* **1**: 667–687.
- Milli S, Palombo MR. 2005. The high-resolution sequence stratigraphy and the mammal fossil record: a test in the Middle–Upper Pleistocene deposits of the Roman Basin (Latium, Italy). *Quaternary International* **126–128**: 251–270.
- Moullé PE, Echaussoux A, Lacomat F. 2006. Taxonomie du grand canidé de la grotte du Vallonnet (Roquebrune-Cap-Martin Alpes-Maritimes). *Anthropologie* **110**: 832–836.
- Pandolfi L. 2013. Rhinocerotidae (Mammalia Perissodactyla) from the Middle Pleistocene site of Ponte Milvio Central Italy. *Bollettino della Società Paleontologica Italiana* **52**: 219–229.
- Pandolfi L, Marra F. 2015. Rhinocerotidae (Mammalia, Perissodactyla) from the chrono-stratigraphically constrained Pleistocene deposits of the urban area of Rome (Central Italy). *Geobios* **48**: 147–167.
- Pandolfi L, Petronio C, Salari L. 2011. *Bos primigenius* Bojanus, 1827 from the early Late Pleistocene deposit of Avetrana (Southern Italy) and the variation in size of the species in Southern Europe: preliminary report. *Journal of Geological Research* **2011**, ID 245408, DOI: 10.1155/2011/245408
- Pandolfi L, Tagliacozzo A. 2015. *Stephanorhinus hemitoechus* (Mammalia, Rhinocerotidae) from the Late Pleistocene of Valle Radice (Sora Central Italy) and re-evaluation of the morphometric variability of the species in Europe. *Geobios* **48**: 169–191.
- Peccerillo A. 2005. *Plio-Quaternary Volcanism in Italy: Petrology Geochemistry Geodynamics*. Springer-Verlag: Berlin.
- Petronio C, Bellucci L, Martinetto E *et al.* 2011. Biochronology and palaeoenvironmental changes from the Middle Pliocene to the Late Pleistocene in Central Italy. *Geodiversitas* **33**: 485–517.
- Petronio C, Sardella R. 1999. Biochronology of the Pleistocene mammal fauna from Ponte Galeria (Rome) and remarks on the Middle Galerian faunas. *Rivista Italiana di Paleontologia e Stratigrafia* **105**: 155–164.
- Piperno M. 1992. Il Paleolitico inferiore. In *Italia Preistorica*, Guidi A, Piperno M (eds). Laterza: Bari 139–169.
- Rivera TA, Storey M, Schmitz MD *et al.* 2013. Age intercalibration of  $^{40}\text{Ar}/^{39}\text{Ar}$  sanidine and chemically distinct U/Pb zircon populations from the Alder Creek Rhyolite Quaternary geochronology standard. *Chemical Geology* **345**: 87–98.
- Servizio Geologico d'Italia. 1970. *arta Geologica dell'Italia a scala 1:100:000 Foglio 144 Palombara Sabina*.
- Sottili G, Palladino DM, Marra F *et al.* 2010. Geochronology of the most recent activity in the Sabatini Volcanic District, Roman Province, central Italy. *Journal of Volcanology and Geothermal Research* **196**: 20–30.
- Sottili G, Palladino DM, Zanon V. 2004. Plinian activity during the early eruptive history of the Sabatini Volcanic District, Central Italy. *Journal of Volcanology and Geothermal Research* **135**: 361–379.
- Van der van der Made J. 2011. Biogeography and climatic change as a context to human dispersal out of Africa and within Eurasia. *Quaternary Science Reviews* **30**: 1353–1367.
- Villa P. 2001. Early Italy and the colonization of Western Europe. *Quaternary International* **75**: 113–130.